Available online at www.sciencedirect.com

ScienceDirect

Mendeleev Commun., 2022, **32**, 198–201

Mendeleev Communications

Ligand-to-ligand charge transfer state in lanthanide complexes containing π-bonded antenna ligands

Daniil A. Bardonov,[a,b] Lada N. Puntus,[a,c] Ilya V. Taidakov,[d] Evgenia A. Varaksina,[d] Konstantin A. Lyssenko,[e,f] Ilya E. Nifant'ev[a,b,e] and Dmitrii M. Roitershtein*[a,b,g]

[a] *A. V. Topchiev Institute of Petrochemical Synthesis, Russian Academy of Sciences, 119991 Moscow, Russian Federation. E-mail: roiter@yandex.ru*
[b] *National Research University Higher School of Economics, 101000 Moscow, Russian Federation*
[c] *V. A. Kotel'nikov Institute of Radioengineering and Electronics, Russian Academy of Sciences, 141190 Fryazino, Moscow Region, Russian Federation*
[d] *P. N. Lebedev Physical Institute, Russian Academy of Sciences, 119991 Moscow, Russian Federation*
[e] *Department of Chemistry, M. V. Lomonosov Moscow State University, 119991 Moscow, Russian Federation*
[f] *G. V. Plekhanov Russian University of Economics, 117997 Moscow, Russian Federation*
[g] *N. D. Zelinsky Institute of Organic Chemistry, Russian Academy of Sciences, 119991 Moscow, Russian Federation*

DOI: 10.1016/j.mencom.2022.03.015

To design luminescent lanthanide complexes containing both π- and σ-bonded antenna ligands in the coordination sphere, we synthesized 2,2′-bipyridine complexes of Nd, Tb and Gd with tri- and tetraphenyl substituted cyclopentadienyl ligands: [$Cp^{Ph_3}LnCl_2$(bipy)(THF)] (Cp^{Ph_3} = 1,2,4-triphenylcyclopentadienyl, bipy = 2,2′-bipyridine) and [$Cp^{Ph_4}LnCl_2$(bipy)(THF)] (Cp^{Ph_4} = tetraphenylcyclopentadienyl). Their crystal structures were determined by X-ray diffraction analysis. Optical spectroscopic and crystallographic data indicate the presence of a ligand-to-ligand charge transfer state.

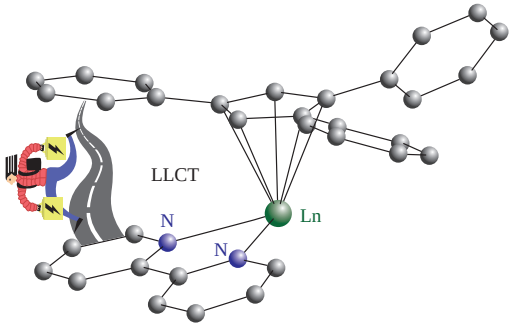

Keywords: lanthanide complexes, Cp ligand, NIR luminescence, crystal structure, charge transfer state.

Dedicated to Academician O. M. Nefedov on the occasion of his 90th birthday

Most lanthanide ions are luminescent with a narrow emission line.[1,2] To improve the quantum yield of the Ln^{3+} ion photoluminescence, researchers generally used indirect excitation of the Ln^{3+} ion. The latter is commonly referred to as the 'antenna' effect.[3] Recently, a new approach to design highly luminescent Ln coordination compounds has been developed based on a π-type ligand, polyphenyl-substituted cyclopentadienyl.[4] The maximum quantum yield of the Tb^{III} ion photoluminescence in the complex with the tetraphenylcyclopentadienyl (Cp^{Ph_4}) ligand was 60%, but in some complexes, it was only 10%. A standard way to improve the luminescence properties of lanthanide complexes is to use auxiliary ligands, which can either prevent vibrational relaxation-based luminescence quenching or serve as an additional 'antenna'. An example of such a design was recently implemented in Cp^{Ph_3}–Tb complexes (Cp^{Ph_3} = 1,2,4-triphenylcyclopentadienyl) using 1,3,5-trimethyl-1,3,5-triazacyclohexane (Me_3tach) as an auxiliary ligand which led to a significant increase in the overall quantum yield.[5]

In continuation of this path, an auxiliary ligand, 2,2′-bipyridine (bipy), traditional for Ln complexes, was chosen. 2,2′-Bipyridine has an optimal set of energy levels for effective sensitization of the luminescence of some Ln^{3+} ions and protects them from luminescence quenching based on vibrational relaxation of a solvate molecule in the coordination sphere.[6] Taking all this into account, we have synthesized, structurally characterized and analyzed the optical spectral properties for two series of Ln complexes containing both π- and σ-antennas, namely, complexes of (mono)cyclopentadienyl lanthanide dichlorides with the aromatic *N*-heterocyclic 2,2′-bipyridine ligand.

To design luminescent lanthanide complexes containing two different types of antenna ligands in the coordination sphere, we synthesized 2,2′-bipyridine complexes of Nd, Tb and Gd with tri- and tetraphenyl substituted cyclopentadienyl ligands.

Heteroleptic complexes [$Cp^{Ph_3}LnCl_2$(bipy)(THF)] and [$Cp^{Ph_4}LnCl_2$(bipy)(THF)] can be obtained either from the previously isolated {[$Cp^{Ph_3}LnCl_2$(THF)]$_2$KCl(THF)$_n$}[4,7] and 2,2′-bipyridine, or using tri- and tetra-phenylcyclopentadienyl lanthanide dichlorides obtained *in situ* from $LnCl_3(THF)_x$ and the corresponding potassium cyclopentadienide. Using these synthetic methods, complexes [$Cp^{Ph_3}LnCl_2$(bipy)(THF)] (Ln = Nd **1Nd**, Gd **1Gd** and Tb **1Tb**) and [$Cp^{Ph_4}LnCl_2$(bipy)(THF)] (Ln = Nd **2Nd**, Gd **2Gd** and Tb **2Tb**) were obtained (Scheme 1).

The structures of complexes **1Ln** and **2Ln** were established by X-ray diffraction analysis. Complexes from both series with Cp^{Ph_3} and Cp^{Ph_4} ligands are isostructural and crystallize in centrosymmetric space groups *Pbca* and *C*2/*c*, respectively, with one

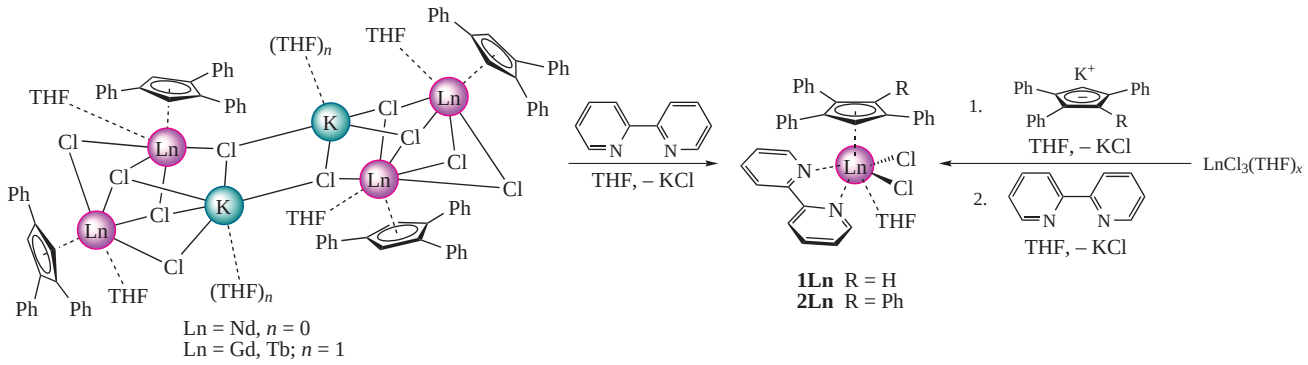

Scheme 1 Synthesis of 2,2′-bipyridine complexes of Nd, Tb and Gd with tri- and tetraphenyl substituted cyclopentadienyl ligands.

independent molecule in the unit cell. In the case of tetraphenyl derivatives, the complexes crystallize with one solvate THF molecule (Figure 1).†

In all studied crystal structures, the Ln^{3+} cations are in a pseudo-octahedral environment with a coordination number of eight if we assume that the Cp^{Ph_x} ligand is one of the vertices (Figure 1). In complexes **1Ln** and **2Ln**, chloride and 2,2′-bipyridine ligands occupy pseudo-equatorial positions, while THF and Cp ligands occupy axial positions. The deviation of the metal atom from the equatorial plane towards the π-ligand is practically the same and amounts to 0.57 Å.

The inspection of molecular geometry has revealed some interesting trends. Considering that the Ln–X distances for different metals depend on the latter's nature due to lanthanide contraction, we will focus our attention on terbium complexes. First, the Tb–N bonds in complexes **1Tb** and **2Tb** are among the shortest for the terbium ion with a coordination number of 8.

Surprisingly, they are almost identical to those in the [Li(THF)][Tb(κ^2-bipy)$_4$] complex with a radical anion form of the 2,2′-bipyridine ligand.[8] More efficient interaction of lone electron pairs of nitrogen with the Ln^{3+} ion in complexes **1Ln** and **2Ln** can be the reason for some weakening of the Ln···π-ligand interaction. Indeed, complex **2Tb** is characterized by a significantly longer Tb–$Cp_{centroid}$ distance (2.49 Å) compared to that in complex **1Tb** (2.45 Å). The latter, in turn, is noticeably longer than in [$Cp^{Ph_4}TbCl_2$(Me$_3$tach)] **3Tb** (2.41 Å).[5] Assuming that the coordination numbers in all these complexes are the same, it is reasonable to suppose that steric hindrance is the main reason for this elongation in complexes **1Ln** and **2Ln**. At the same time, the Tb–Cl bond lengths in complexes **1Tb**–**3Tb** decreases from 2.61 Å in complex **1Tb** to 2.59 Å in complex **3Tb**. From a geometrical point of view, the mutual influence of Cp^{Ph_x} and bipy ligands can occur due to forced contact between two π-systems, the phenyl ring of the Cp^{Ph_x} ligand and the pyridine ring of 2,2′-bipyridine. Indeed, the shortest intramolecular C···C and N···C contacts are 3.18 and 3.20 Å in complex **1Tb**, respectively, and 3.29 Å in complex **2Tb** (Figure 2). Furthermore, this contact leads to a small value of the rotation angle (3.3°) for the phenyl group at position 4, which is unusual for the Cp^{Ph_3} ligand. The Ph rings in the Cp^{Ph_4} ligand in complex **2Ln** are also more coplanar to the Cp ring plane.[4]

Such type of forced intramolecular contact formed by π-systems is well known for [2.2]paracyclophane, for example, and can lead to additional excited states due to charge transfer.[9,10] It should be noted that the strength of such interactions depends on the nature of the lanthanide ions. For example, in complex **1Nd**,

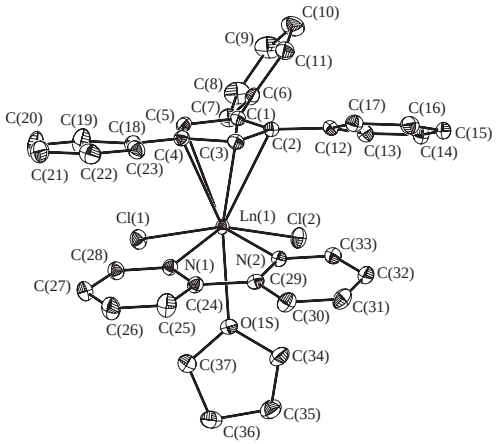

Figure 1 Molecular structure of complexes **1Ln** with thermall ellipsoids at 50% probability level. All hydrogen atoms are omitted for clarity.

† *Crystal data for* **1Gd**. $C_{37}H_{33}Cl_2GdN_2O$, M = 749.80, orthorhombic, space group *Pbca*, T = 100 K, a = 16.6120(6), b = 16.5336(6) and c = 23.4439(8) Å, V = 6439.0(4) Å^3, Z = 8 (Z' = 1). A total of 97528 reflections (θ_{max} = 29°, R_{int} = 0.0309) were collected, and 8558 independent reflections were used for the structure solution and refinement, which converged to R_1 = 0.0231 (for 7067 observed reflections), wR_2 = 0.0568, GOF = 0.925.

Crystal data for **1Nd**. $C_{37}H_{33}Cl_2N_2NdO$, M = 736.79, orthorhombic, space group *Pbca*, T = 100 K, a = 16.669(6), b = 16.586(6) and c = 23.670(8) Å, V = 6544(4) Å^3, Z = 8 (Z' = 1). A total of 69464 reflections (θ_{max} = 29°, R_{int} = 0.0540) were collected, and 8702 independent reflections were used for the structure solution and refinement, which converged to R_1 = 0.0535 (for 6492 observed reflections), wR_2 = 0.0996, GOF = 1.224.

Crystal data for **1Tb**. $C_{37}H_{33}Cl_2N_2OTb$, M = 751.47, orthorhombic, space group *Pbca*, T = 100 K, a = 16.5828(6), b = 16.5328(6) and c = 23.5481(9) Å, V = 6455.9(4) Å^3, Z = 8 (Z' = 1). A total of 31077 reflections (θ_{max} = 22.5°, R_{int} = 0.0540) were collected, and 7400 independent reflections were used for the structure solution and refinement, which converged to R_1 = 0.0438 (for 6005 observed reflections), wR_2 = 0.1070, GOF = 0.959.

Crystal data for **2Gd**. $C_{47}H_{45}Cl_2GdN_2O_2$, M = 898.00, monoclinic, space group $C2/c$, T = 220 K, a = 35.8480(8), b = 11.3038(2) and c = 21.2399(5) Å, β = 109.3858(12)°, V = 8118.8(3) Å^3, Z = 8 (Z' = 1). A total of 59511 reflections (θ_{max} = 29°, R_{int} = 0.0293) were collected, and 10793 independent reflections were used for the structure solution and refinement, which converged to R_1 = 0.0382 (for 9176 observed reflections), wR_2 = 0.0857, GOF = 1.084.

Crystal data for **2Tb**. $C_{47}H_{45}Cl_2N_2O_2Tb$, M = 899.67, monoclinic, space group $C2/c$, T = 220 K, a = 35.8039(15), b = 11.2908(4) and c = 21.2173(11) Å, β = 109.434(2)°, V = 8088.5(6) Å^3, Z = 8 (Z' = 1). A total of 58885 reflections (θ_{max} = 29°, R_{int} = 0.0265) were collected, and 10747 independent reflections were used for the structure solution and refinement, which converged to R_1 = 0.031 (for 9330 observed reflections), wR_2 = 0.0774, GOF = 1.046.

The measurements were performed using a Bruker D8 QUEST diffractometer (graphite monochromated MoKα radiation, ω-scans technique). The structures were solved by dual methods and refined in the anisotropic–isotropic (hydrogen atoms) model.

CCDC 2105264–2105268 contain the supplementary crystallographic data for this paper. These data can be obtained free of charge from The Cambridge Crystallographic Data Centre *via* http://www.ccdc.cam.ac.uk.

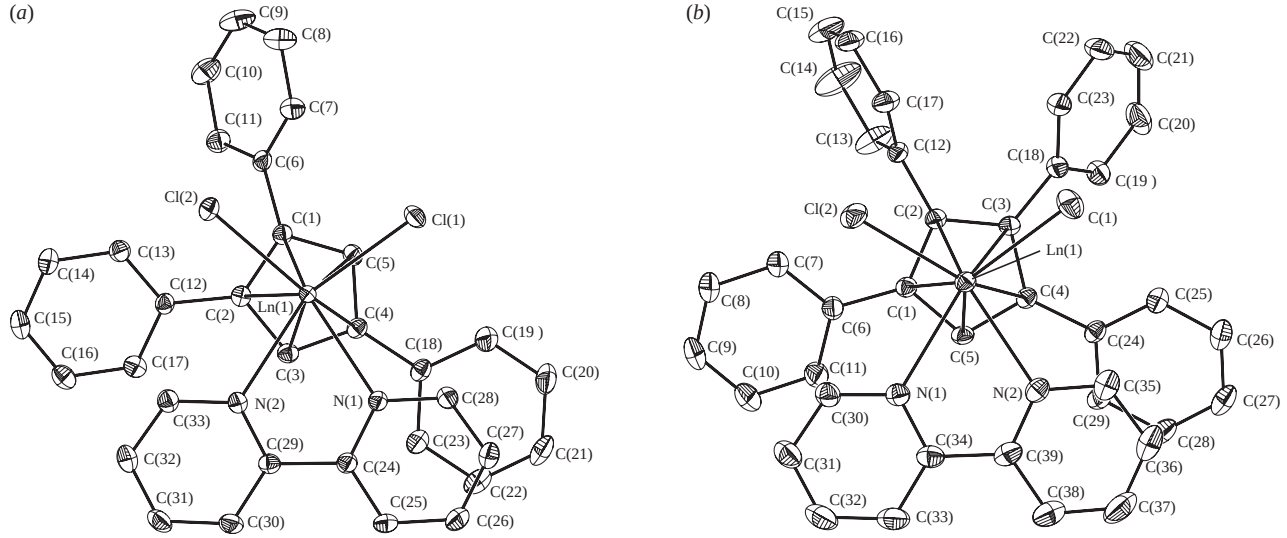

Figure 2 Projections illustrating intramolecular π···π interactions in (*a*) complexes **1Ln** and (*b*) complexes **2Ln**. THF molecules are omitted for clarity.

all of the above intramolecular contacts are slightly longer than in complex **1Tb** due to increased ionic radius.

The synthesized complexes **1Ln** and **2Ln** were investigated by optical spectroscopy. The luminescence spectra of Tb complexes recorded in the range of 470–720 nm upon excitation at Cp transitions do not exhibit characteristic narrow emission bands assigned to the $4f^8$ transitions of the Tb^{3+} ion but only broad luminescence bands. The latter is unexpected, bearing in mind the following. On the one hand, the Tb chloride complex with only one bipy ligand and four coordinated water molecules demonstrated high-intensity luminescence.[5] On the other hand, the Tb complexes containing only the π-bonded antenna ligands Cp^{Ph_3} and Cp^{Ph_4} demonstrated good luminescence characteristics, including the overall quantum yield of photoluminescence (11 and 60%, respectively).[4] However, in complexes **1Tb** and **2Tb** containing phenyl substituted Cp and bipy ligands, strong quenching of the Tb^{3+} ion luminescence is observed, despite the fact that the Tb–N bonds in complexes **1Ln** and **2Ln** are remarkably shorter than usually.

The luminescence excitation spectra of the Tb complexes at low temperature monitored around the peak of the intense $^5D_4 \rightarrow {}^7F_5$ transition of the Tb^{3+} ion at 545 nm exhibit overlapping intense bands extending from 250 to 500 nm [Figure 3(*a*), curve *3*]. Narrow absorption bands assigned to the $4f^8$-intraconfigurational transitions of the Tb^{3+} ion are absent in these spectra. According to published data, the energy of the S_1 state assigned to π–π* transitions of unsubstituted Cp is 270 nm (37037 cm^{-1}), and the introduction of the third and fourth phenyl substituents decreases the energy of this state to 355 nm (28170 cm^{-1}).[4] The energy of the S_1 state assigned to π–π* transitions of coordinated 2,2′-bipyridine is 330 nm (30300 cm^{-1}).[11] In the considered excitation spectra, the noted bands with maxima at 330 and 360 nm are observed, as well as a band at 490 nm (20410 cm^{-1}). Consequently, there are S_1 states assigned to π–π* transitions of coordinated 2,2′-bipyridine (330 nm) and the Cp ligand (360 nm). The third broad band with a maximum at 490 nm is also found in the excitation spectra of the Gd and Nd complexes; therefore, it is logical to assume that it originates from ligands.

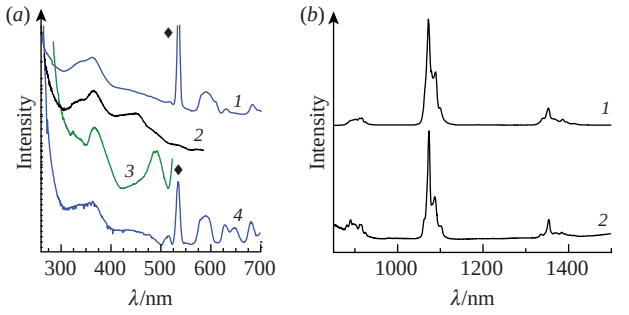

Figure 3 (*a*) Luminescence excitation spectra of (*1*) complex **Nd1**, (*2*) complex **Gd1** and (*3*) complex **Tb1** at 77 K and (*4*) complex **Nd2** at 300 K. The symbol ♦ denotes the second order artefact of λ_{reg}. (*b*) Luminescence spectra of (*1*) complex **Nd1** and (*2*) complex **Nd2** at 300 K (λ_{exc} = 340 nm).

Earlier, in the luminescence excitation spectra of Ln complexes with the Cp^{Ph_3} and Cp^{Ph_4} ligands, a low-lying excited state was found in the range of 410−430 nm, and it was tentatively assigned to the intraligand charge transfer (ILCT) state.[4] The origin of this state was due to the K···π interaction, in which the K^+ cation participates in additional coordination with the phenyl ring of the Cp ligands. Such K···π interaction causes an additional charge redistribution from the Cp system to the phenyl group and results in the ILCT state. Thus, it is reasonable to assume that the same situation is realized in complexes **1Ln** and **2Ln**. According to X-ray diffraction data, the mutual arrangement of 2,2′-bipyridine and the phenyl group may promote the appearance of the ligand-to-ligand charge transfer (LLCT) state. Therefore, a broad band centered at 490 nm in the excitation spectra can be tentatively assigned to the LLCT state. It is important to emphasize that the ILCT state is well known for lanthanide complexes with ligands containing donor and acceptor moieties,[12,13] while the LLCT state is found for the lanthanide system for the first time according to the best of our knowledge.

To estimate whether the geometric criteria for intramolecular charge transfer are valid for these complexes, we performed TD-DFT calculations for complex **1Tb**. According to these calculations, the lowest energy transitions $T_1 \rightarrow S_0$ and $S_1 \rightarrow S_0$ with the energy of *ca.* 440 nm are HOMO-to-LUMO transitions (Figure 4). As one can see, the HOMO orbital mainly consists of Cp-ring orbitals and is partially coplanar to its phenyl groups. The main contribu-

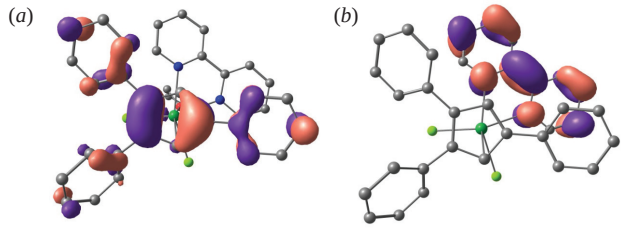

Figure 4 Visualization of (*a*) the HOMO and (*b*) the LUMO in complex **1Tb**. The THF molecule is omitted for clarity.

tion to LUMO is made by the bipy ligand. Thus, these transitions correspond to an energy transfer from the Cp^{Ph_3} anion to 2,2′-bipyridine and can be considered a ligand-to-ligand charge transfer transition.

According to the generally accepted concept, sensitized luminescence in Ln-containing systems results from energy migration from the singlet excited state S_1 of the ligand to its triplet state T_1 and, finally, to the excited levels of the lanthanide ion. In the case of complexes containing the Tb^{3+} ion, the probability of back energy transfer (BET) process from the $^5D_4$ level to the T_1 level of the ligand is high when the triplet state of the ligand has energy close to the excited Tb^{3+} levels. Thus, the presence of a low-lying excited state with the energy of ~490 nm (20410 cm^{-1}) when the energy of the $^5D_4$ level is the same leads to the luminescence quenching of the Tb^{3+} ion due to the BET process.

Since the resonance level energy of the Nd^{3+} ion is remarkably lower [870 nm (11500 cm^{-1})] than that of the Tb^{3+} ion [490 nm (20410 cm^{-1})], BET does not occur, and typical luminescence of the Nd^{3+} ion should be observed. Indeed, neodymium complexes **1Nd** and **2Nd** exhibit luminescence in the NIR region at both 77 and 300 K [Figure 3(*b*)]. The observed *f*–*f* emission bands correspond to the typical electronic transitions of the Nd^{3+} ion, namely, $^4F_{3/2} \rightarrow {}^4I_{9/2}$ (870−930 nm), $^4F_{3/2} \rightarrow {}^4I_{11/2}$ (1040−1100 nm) and $^4F_{3/2} \rightarrow {}^4I_{13/2}$ (1320−1400 nm). The luminescence decay curves of the Nd complexes were adjusted with a single exponential function. The lifetime values (τ) of the $^4F_{3/2}$ emitting level are 0.46 and 0.42 μs for complexes **1Nd** and **2Nd**, respectively. The luminescence excitation spectra contain both absorption bands of the ligands and *f*–*f** transitions [Figure 3(*a*), curves *1* and *4*].

Thus, we first hypothesized and proved theoretically and experimentally the existence of ligand-to-ligand charge transfer in the lanthanide complex and discussed LLCT in the energy migration process. The lack of such intramolecular ligand–ligand interaction in Ln complexes is explained solely by geometric constraints arising from the parallel arrangement of ligands in the case of common σ-bonded antenna ligands. In contrast, for the π-bonded antenna ligand, it is evident that the pseudo-octahedral environment promotes LLCT and, therefore, it is necessary to take into account its possible presence and role in sensitizing the Ln ion luminescence. Finally, one has to keep in mind that such LLCT can be important for designing new materials for NLO applications.

This work was supported by the Russian Science Foundation (grant no. 17-13-01357). The authors acknowledge support from the Development Program of the M. V. Lomonosov Moscow State University for providing access to single-crystal X-ray diffraction.

Online Supplementary Materials

Supplementary data associated with this article can be found in the online version at doi: 10.1016/j.mencom.2022.03.015.

References

1 (*a*) J.-C. G. Bünzli and S. V. Eliseeva, in *Comprehensive Inorganic Chemistry II: From Elements to Applications*, 2nd edn., eds. J. Reedijk and K. Poeppelmeier, Elsevier, Amsterdam, 2013, vol. 8, pp. 339–398; (*b*) S. V. Eliseeva and J.-C. G. Bünzli, *New J. Chem.*, 2011, **35**, 1165; (*c*) J.-C. G. Bünzli and S. V. Eliseeva, *Chem. Sci.*, 2013, **4**, 1939; (*d*) *Luminescence of Lanthanide Ions in Coordination Compounds and Nanomaterials*, ed. A. de Bettencourt-Dias, John Wiley & Sons, Ltd., Chichester, UK, 2014.

2 (*a*) J.-C. G. Bünzli, in *Handbook on the Physics and Chemistry of Rare Earths*, eds. J.-C. G. Bünzli and V. K. Pecharsky, Elsevier, Amsterdam, 2016, vol. 50, pp. 141–176; (*b*) O. K. Farat, A. V. Kharcheva, V. A. Ioutsi, N. E. Borisova, M. D. Reshetova and S. V. Patsaeva, *Mendeleev Commun.*, 2019, **29**, 282; (*c*) J.-C. G. Bünzli, *Acc. Chem. Res.*, 2006, **39**, 53; (*d*) G. Zucchi, R. Scopelliti, P.-A. Pittet, J.-C. G. Bünzli and R. D. Rogers, *J. Chem. Soc., Dalton Trans.*, 1999, 931.

3 (*a*) S. I. Weissman, *J. Chem. Phys.*, 1942, **10**, 214; (*b*) R. E. Whan and G. A. Crosby, *J. Mol. Spectrosc.*, 1962, **8**, 315; (*c*) G. A. Crosby, R. E. Whan and R. M. Alire, *J. Chem. Phys.*, 1961, **34**, 743; (*d*) G. A. Crosby, R. E. Whan and J. J. Freeman, *J. Phys. Chem.*, 1962, **66**, 2493; (*e*) S. V. Eliseeva and J.-C. G. Bünzli, *Chem. Soc. Rev.*, 2010, **39**, 189; (*f*) D. Parker, *Chem. Soc. Rev.*, 2004, **33**, 156.

4 D. M. Roitershtein, L. N. Puntus, A. A. Vinogradov, K. A. Lyssenko, M. E. Minyaev, M. D. Dobrokhodov, I. V. Taidakov, E. A. Varaksina, A. V. Churakov and I. E. Nifant'ev, *Inorg. Chem.*, 2018, **57**, 10199.

5 D. A. Bardonov, P. D. Komarov, V. I. Ovchinnikova, L. N. Puntus, M. E. Minyaev, I. E. Nifant'ev, K. A. Lyssenko, V. M. Korshunov, I. V. Taidakov and D. M. Roitershtein, *Organometallics*, 2021, **40**, 1235.

6 (*a*) L. N. Puntus, K. A. Lyssenko, I. S. Pekareva and J.-C. G. Bünzli, *J. Phys. Chem. B*, 2009, **113**, 9265; (*b*) J.-C. G. Bünzli and C. Piguet, *Chem. Soc. Rev.*, 2005, **34**, 1048; (*c*) C. Janiak, *J. Chem. Soc., Dalton Trans.*, 2000, 3885.

7 M. E. Minyaev, A. A. Vinogradov, D. M. Roitershtein, R. S. Borisov, I. V. Ananyev, A. V. Churakov and I. E. Nifant'ev, *J. Organomet. Chem.*, 2016, **818**, 128.

8 R. L. Halbach, G. Nocton, J. I. Amaro-Estrada, L. Maron, C. H. Booth and R. A. Andersen, *Inorg. Chem.*, 2019, **58**, 12083.

9 K. A. Lyssenko, A. A. Korlyukov and M. Yu. Antipin, *Mendeleev Commun.*, 2005, **15**, 90.

10 L. N. Puntus, E. V. Sergeeva, D. Yu. Antonov, K. Yu. Suponitsky, I. Rau, F. Kajzar and K. A. Lyssenko, *Mol. Cryst. Liq. Cryst.*, 2017, **655**, 16.

11 L. N. Puntus, *Helv. Chim. Acta*, 2009, **92**, 2552.

12 (*a*) A. D'Aléo, F. Pointillart, L. Ouahab, C. Andraud and O. Maury, *Coord. Chem. Rev.*, 2012, **256**, 1604; (*b*) L. N. Puntus, V. F. Zolin, V. A. Kudryashova, V. I. Tsaryuk, J. Legendziewicz, P. Gawryszewska and R. Szostak, *Phys. Solid State*, 2002, **44**, 1440 (*Fiz. Tverd. Tela*, 2002, **44**, 1380).

13 (*a*) L. N. Puntus, V. F. Zolin, T. A. Babushkina and I. B. Kutuza, *J. Alloys Compd.*, 2004, **380**, 310; (*b*) A. D'Aléo, J. Xu, E. G. Moore, C. J. Jocher and K. N. Raymond, *Inorg. Chem.*, 2008, **47**, 6109; (*c*) C. Yang, L.-M. Fu, Y. Wang, J.-P. Zhang, W.-T. Wong, X.-C. Ai, Y.-F. Qiao, B.-S. Zou and L.-L. Gui, *Angew. Chem., Int. Ed.*, 2004, **43**, 5010; (*d*) G. A. Hebbink, S. I. Klink, L. Grave, P. G. B. Oude Alink and F. C. J. M. van Veggel, *ChemPhysChem*, 2002, **3**, 1014.

Received: 30th August 2021; Com. 21/6668